

## Investigation on Characteristics of Metamaterials by Using Metallic Rod Structure for Antenna Engineering

**Abstract.** In this research, the investigation of metallic rod type metamaterials is presented. In the study, the simulation and numerical analysis are performed to analyze the classification of metamaterials when the metallic rods are arranged in various patterns, including permittivity, permeability and reflection index. From the simulation and numerical results, it was found that metallic rod is classified in epsilon near zero characteristics when metallic rods are arranged with double and three layers. Electromagnetic properties of proposed structure are electromagnetic band gap and partially reflective surface at the designed frequency. In addition, the band gap of the proposed structure is studied. The proper layer number and pattern of metallic rods structure can control the operating frequency band. The structure can be future applied such as improving characteristic of antenna and electromagnetic interference.

**Streszczenie.** W pracy przedstawiono badania metamateriałów typu metalicznego pręta. W badaniu przeprowadzono symulację i analizę numeryczną w celu przeanalizowania klasyfikacji metamateriałów, gdy metalowe pręty są ułożone w różne wzory, w tym przenikalność, przepuszczalność i współczynnik odbicia. Na podstawie symulacji i wyników numerycznych stwierdzono, że pręt metalowy jest klasyfikowany w charakterystyce epsilon bliskiej zeru, gdy pręty metalowe są ułożone z podwójną i trzema warstwami. Właściwości elektromagnetyczne proponowanej konstrukcji to pasmo wzbronione elektromagnetyczne oraz częściowo odbijająca powierzchnia przy projektowanej częstotliwości. Dodatkowo badane jest pasmo wzbronione proponowanej struktury. Właściwa liczba warstw i wzór struktury metalowych prętów może sterować pasmem częstotliwości pracy. Struktura może być w przyszłości zastosowana np. do poprawy charakterystyki anteny i zakłóceń elektromagnetycznych. (Badanie właściwości metamateriałów przy użyciu metalicznej struktury prętów w inżynierii antenowej)

**Keywords:** Metallic Rod, Metamaterials, Epsilon Near Zero, Antenna Engineering.

**Słowa kluczowe:** metamateriały, pręt, antena

### Introduction

Over the years, artificial electromagnetic materials which has different property from nature known as "Metamaterial", has received great deal of attention form 2008 to present [1] – [9]. All natural materials such as glass, diamond, and such have positive electrical permittivity, magnetic permeability and an index of refraction. It comprises of periodic or non-periodic structure. Metamaterials are generally specified by the parameter of structure design. The characteristic of metamaterials is shown in the effective macroscopic behavior. Early-stage researchers researches a negative refraction index, based on super lens technique. It can magnify a picture that its resolution is higher than a limited of general lens. In addition, negative refraction index is also called left hand metamaterials [10] – [11]. The electromagnetic metamaterials have various types such as negative refractive index, electromagnetic bandgap (EBG) metamaterials, double positive medium and so on. The metamaterials are classified by permittivity ( $\epsilon$ ) and permeability ( $\mu$ ), the equivalent permittivity and permeability are primarily dependent on the geometrical properties of an inclusion shape and mutual distance between the lattice constant. Therefore, it is possible to tailor the electromagnetic response of the inclusions almost arbitrarily and achieve exotic values of equivalent permittivity and permeability that cannot be found in nature. A part from natural double-positive materials (DPS), there are also materials that have either negative permittivity or negative permeability (SNG). Whereas, the negative permittivity materials are called epsilon negative medium (ENG) and the negative permeability materials are called mu negative medium (MNG). Furthermore, zero refractive index or near zero refractive index materials are described in antenna engineering that are classified in three types.

1) When a permeability greater than or equal to one ( $\mu \geq 1$ ), this case is called epsilon near zero (ENZ).

2) When a permittivity greater than or equal to one ( $\epsilon \geq 1$ ), this case is called mu near zero (MNZ).

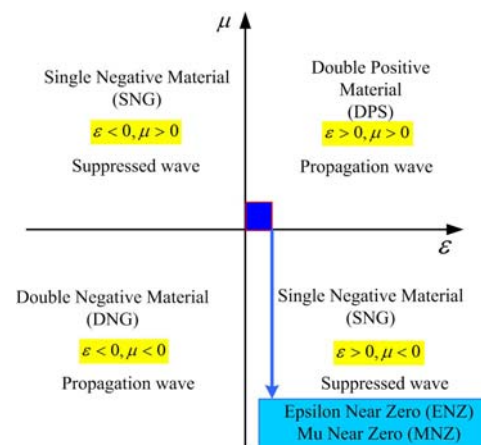


Fig.1. Classification of metamaterials.

3) When a permeability and a permittivity are zero ( $\mu = \epsilon = 0$ ), this case is called double zero index or mu-epsilon near zero.

The classification of metamaterials is illustrated in Fig. 1.

Moreover, the antenna is another possible application which uses metamaterials to increase performance of the antenna system [12] – [16]. Consideration to metamaterial types applied in antenna engineering, the electromagnetic band gap (EBG) and partially reflective surface (PRS) based on electromagnetic metamaterials are widely used in antenna design to enhance the natural performance of the traditionally antenna. EBG is a periodic structure, consists of dielectric and metallo-dielectric materials. It is capable of the radiation deterrence in a specific direction and frequency. The diversity of EBG structure that is applied for the antenna application can be also divided in three categories which are high impedance surface, artificial surface and high directive resonator antenna. High impedance surface is a new type of metallic

electromagnetic structure. It is a planar array of continuous metallic periodic cell surfaces able to suppress surface waves, which cause multipath interference and backward radiation in a narrow bandwidth near the cell resonance [17] - [18]. Artificial surfaces are artificial magnetic conductors (AMC) and reactive surfaces to design low profile antenna. [19] - [20]. A resonator antenna is designed base on the basis of creating detects in a uniform EBG structure. It is composed of a complex artificial surface and a metallic ground plane. Moreover, a primary radiation source such as microstrip patch antennas, horn antennas, dipole antennas, and so on, the EBG structure can be configured as a superstrate. The main goal of using EBG is to improve the primary radiating efficiency. The structure of various forms of EBG can be used in the design of high directive gain resonator antenna. [21] - [24]. In addition, PRS works as a medium in form of a superstrate. Fig. 2 demonstrates the propagation of electromagnetic fields which are passed through the medium, the reflection and refraction wave occurs. In this case, the electromagnetic waves propagate along x direction. The advantage of PRS is increasing the amplitude of electromagnetic wave that is transmitted to PRS surface.

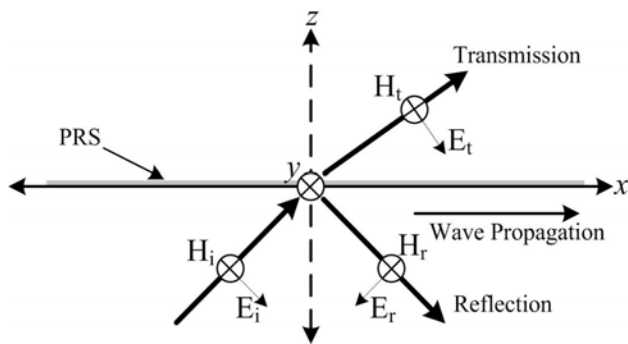


Fig.2. Electromagnetic Wave propagation of PRS.

As mention previously, the following section of the paper presents the microwave metamaterials types when the metallic rod structure is modified. The electromagnetic band gap (EBG) and partially reflective surface (PRS) structure based on electromagnetic metamaterials are described. The properties of a unit cell model for the metallic rod and a cavity model composed of a unit cell and its image is simulated in Section 2. The classification of microwave metamaterials when metallic rod structure is formed in different patterns are discussed in Section 3. Finally, the characteristics of the proposed metamaterials are concluded.

### Unit cell model of metallic rod

To design the metamaterials, the image theory is applied. A cavity consisted of the metallic rod and its image that is resonated at the resonant frequency as the application that want to be applied. Because the size of the exciting feed is considered much smaller than that the EBG superstrate and the reflector plane, the effect of the small feed antenna on the resonant cavity can be ignored [25]. Therefore, a unit cell is surrounded by four periodic boundaries and a unit cell model is shown in Fig. 3(a). This model can be used to evaluate the transmission and reflection amplitude and phase of the proposed unit cell, under the normal incidence. Fig. 3(b) illustrates the cavity model that it has a single cell of the periodic structure and its image surrounded by four periodic boundaries. For normal incidence, the periodic boundaries surrounding the unit cell or the unit cavity can be replaced by the PEC

(perfect electric conductor) and PMC (perfect magnetic conductor) walls.

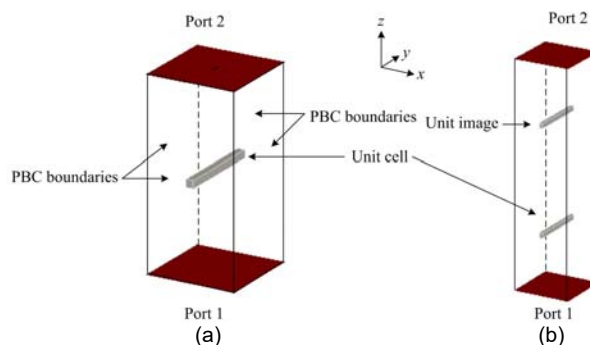


Fig.3. (a) A unit cell model for the EBG and (b) a cavity model composed of a unit cell and its image

In the case shown in Fig. 3(a), a metallic rod performs as a unit cell. The boundary perpendicular to axis x should be set as PEC walls and those perpendicular to axis y should be PMC walls. Waveguide ports are located on two sides of the model. To analyze the transmission and reflection coefficient through the equivalent cavity model, shown in Fig. 3(b), the EBG and its image are included in the cavity model.

### Simulated and calculated results of metallic rod characteristic

In this section, the simulation and numerical are performed by focusing on microwave frequency band of 1 to 4 GHz. Furthermore, metallic rod unit cell is classified in three cases which are single layer, double layers, and three layers as follows.

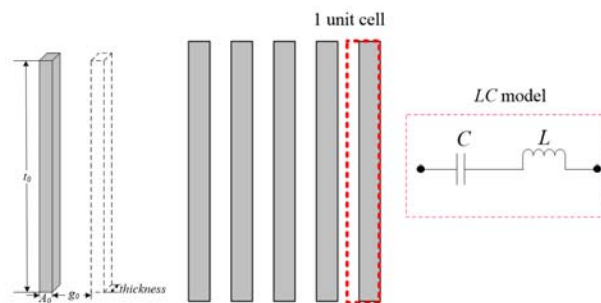


Fig.4. A unit cell of single layer metallic rod.

### Single layer of metallic rod

Unit cell of metallic rod is a primary simulation of the metamaterials design as shown in Fig. 4. A unit cell defined by parameters  $A_0$ ,  $g_0$ , and  $t_0$  and an aluminium rod is surrounded by four periodic boundaries. The parameters are optimized as plotted in Fig. 5 to analyze the reflection phase that can be reflected partial wave, so  $A_0$ ,  $g_0$ , and  $t_0$  are  $0.09\lambda$ ,  $0.25\lambda$ , and  $0.5\lambda$ , respectively. It seems that the resonant frequency is determined by the parameter of the aluminium rod structure, especially by the  $A_0$  and  $g_0$  of rod structure. This model can be estimated the transmission and the reflection coefficient of the aluminium rod structure as plotted in Fig. 6. Consideration of  $S_{11}$  and  $S_{21}$  at 2.1 GHz concludes that the aluminium rod can be partially reflected wave. The reflection phase in Fig. 6(b). The advantage of this structure can be used to superstate for improving the directive gain of the exciting feed antenna in its own polarization. However, the allowed bandwidth is mostly narrow.

More interestingly, the S-parameters are used to calculate the permittivity ( $\epsilon$ ), permeability ( $\mu$ ), and refraction index ( $n$ ) of the aluminium rod structure, and the results. Initially, the basic equations used to determine the  $\epsilon$ ,  $\mu$ , and  $n$  are shown below: [26]

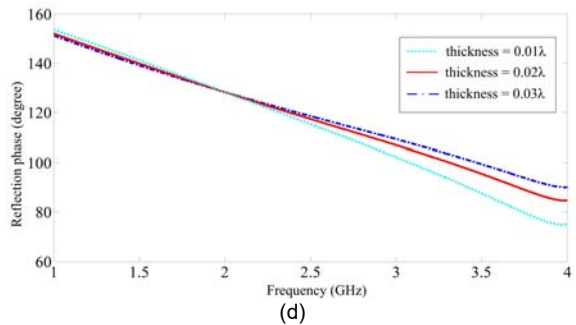
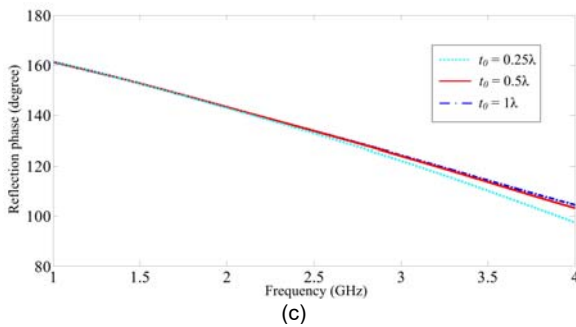
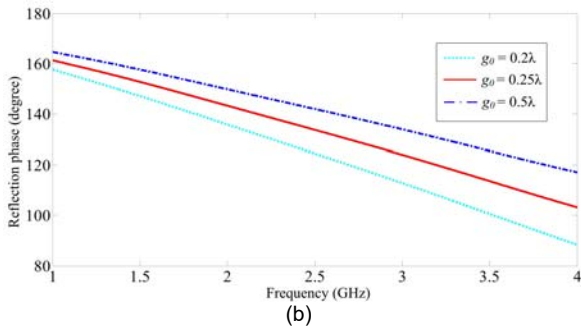
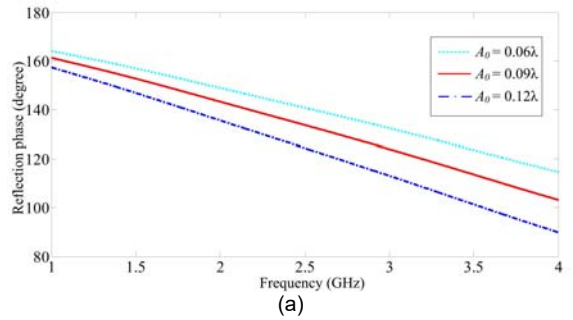


Fig.5. Optimization of EBG parameters (a)  $A_0$ , (b)  $g_0$ , (c)  $t_0$ , and (d) thickness.

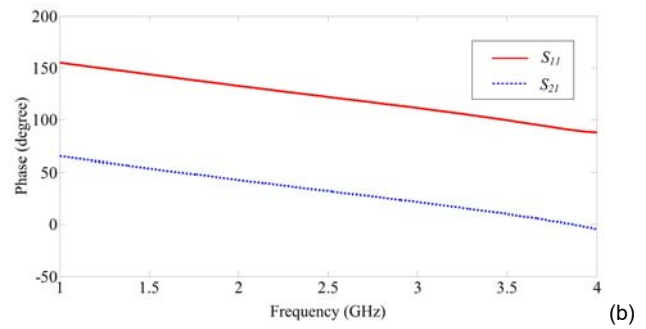
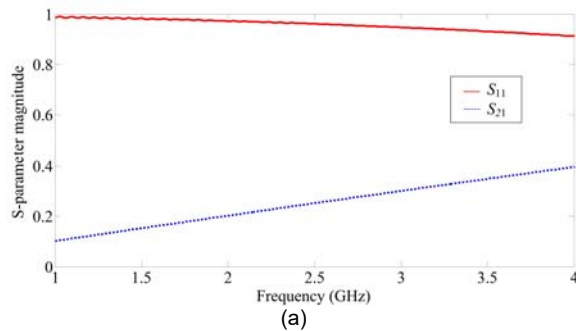


Fig.6. S-parameter of single layer (a) magnitude and (b) phase.

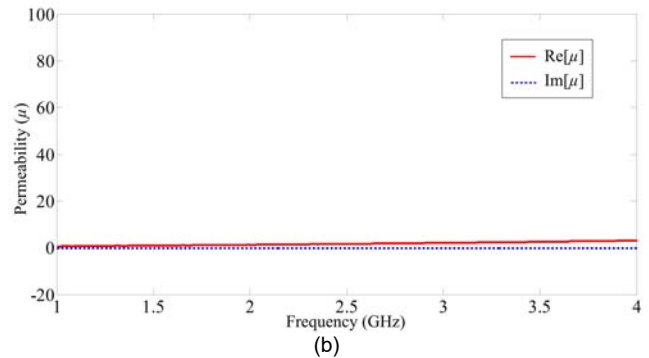
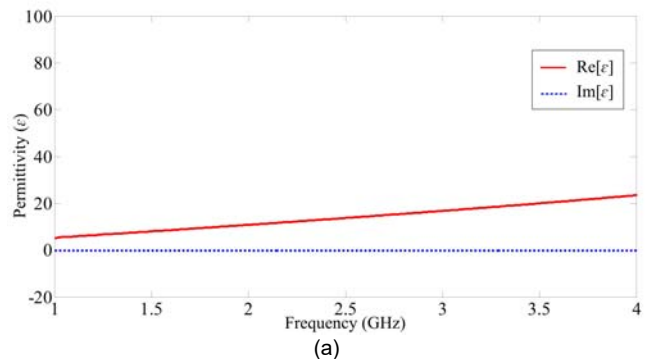
$$(1) \quad \epsilon_r \approx \frac{2}{jk_0 d} \frac{1-v_1}{1+v_1}$$

$$(2) \quad \mu_r \approx \frac{2}{jk_0 d} \frac{1-v_2}{1+v_2}$$

$$(3) \quad n = \pm \sqrt{\epsilon \mu}$$

where:  $v_1 = S_{21} + S_{11}$ ,  $v_2 = S_{21} - S_{11}$ ,  $k_0 = \omega/c$ ,  $\omega$  is radiation frequency,  $d$  is dielectric thickness,  $c$  is speed of light.

The permittivity and permeability at the resonant frequency of this structure is depicted in Fig. 7 with the value of 11.46 and 1.4, respectively. The aluminium rod is classified in a medium with both permittivity and greater than zero ( $\epsilon > 0$ ,  $\mu > 0$ ). Referring to Fig. 7 (c) concluded that the refraction index is 4.01. Therefore, the wave propagation incident upon a plane surface separating two media is refracted upon entering the second medium if the incident wave is oblique to the surface. The incident angle is related to the refraction angle by the simple relationship known as Snell's law.



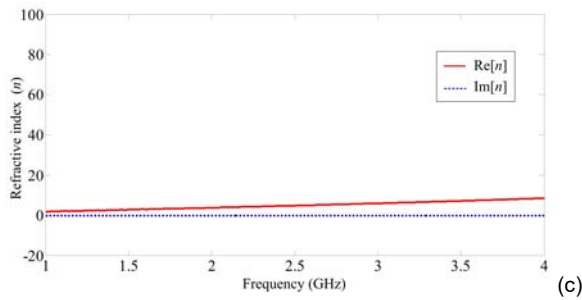


Fig.7. Calculated results of single layer unit cell aluminium rod (a)  $\epsilon_r$ , (b)  $\mu_r$ , and (c)  $n$

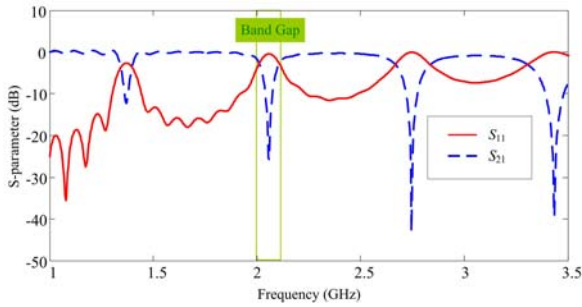


Fig.8. The band gap of single layer.

One characteristic of the electromagnetic band gap (EBG) based on metamaterials is to prohibit the wave propagation whose frequency belongs to the material band gap. The second characteristic property is to allow electromagnetic modes to exist within the forbidden frequency band by using the cavity model. Let us now analyze the transmission and reflection coefficient, assuming the cavity height ( $h$ ) is adjusted to control the band gap of single layer which is 67.46 mm. This S-parameter is plotted in Fig. 8 and indicated that the cavity resonance frequencies is 2 GHz to 2.1 GHz.

### Double layers of metallic rod

In this research, double layers of EBG superstrate are divided into two cases which are cross polarization and co-polarization of metallic rod.

#### Case 1 : Cross polarization of metallic rod

Both the EBG polar H and EBG polar V are considered and shown in Fig. 9. This model can estimate the transmission and the reflection wave of the EBG structure as plotted in Fig. 10(a). It concludes that the aluminium rod can be partially reflected wave. The reflection phase in.

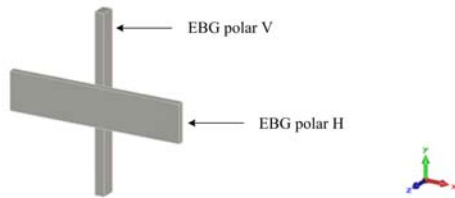


Fig.9. A unit cell of double layers with cross polarized EBG.

Fig. 10(b) is performed that the allowed bandwidth is mostly narrow. Referring to Fig. 11 that shows the aluminium rods which are classified in a medium with epsilon near zero (ENZ). The permittivity and permeability at the resonant frequency are 0.14 ( $0 < \epsilon < 1$ ) and 6.5, respectively, so the reflection index of double layers EBG with cross polarization is about 0.95. From Equation (4.5), if the permittivity is near zero and the reflection index is closed to zero, so the directivity enhancement in this

medium is based on the phenomenon of geometrical optics and Snell's law. [27] The exiting ray from the substrate will be normal to the surface.

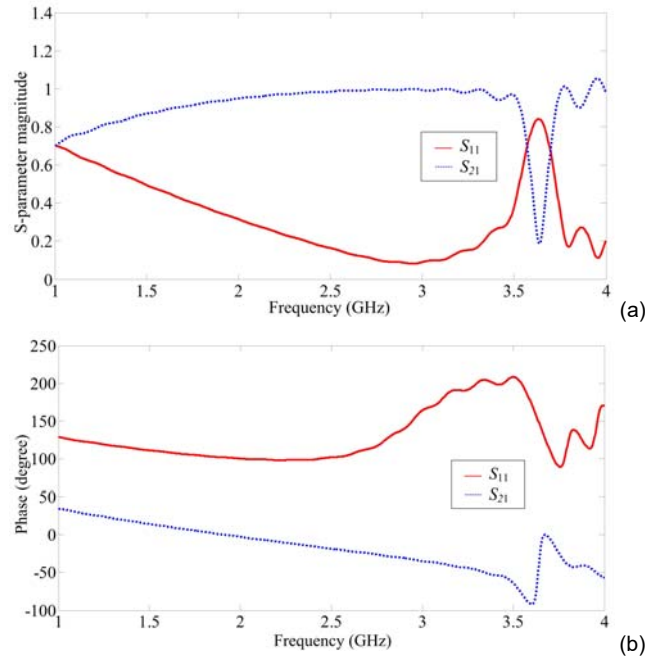


Fig.10. S-parameter of a cross polarized double layer EBG (a) magnitude and (b) reflection phase.

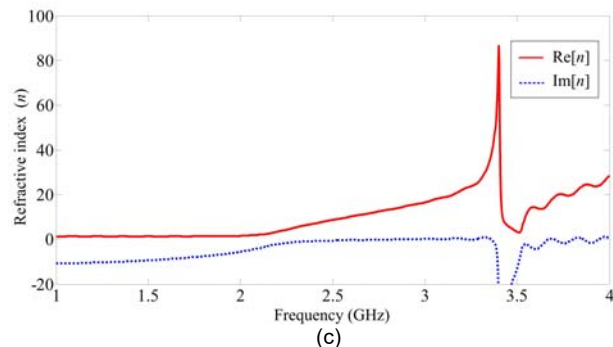
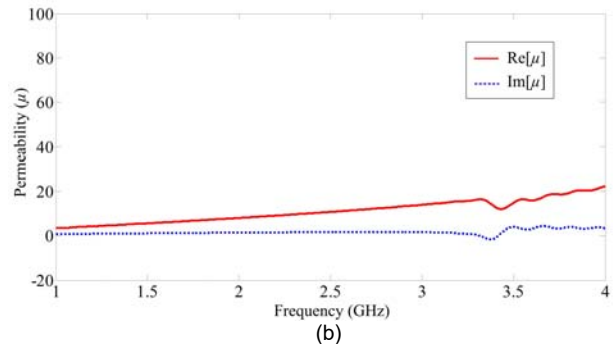
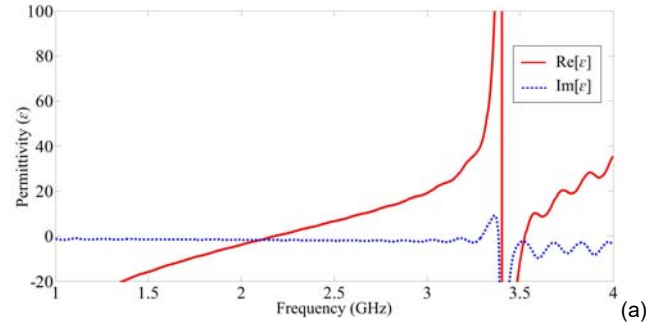


Fig. 11. Calculated results of the double layers with cross polarized EBG (a)  $\epsilon_r$ , (b)  $\mu_r$ , and (c)  $n$

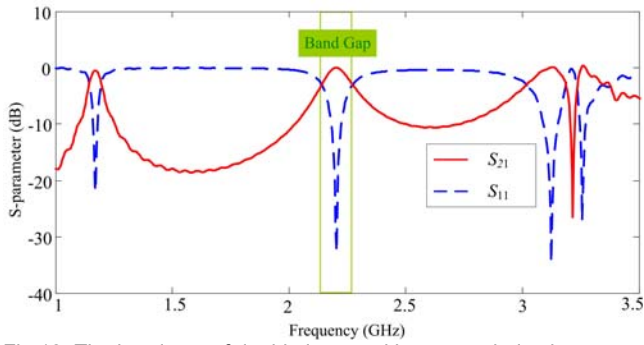


Fig. 12. The band gap of double layers with cross polarization

The band gap of the cross polarized EBG is obtained by using the cavity model. Assuming the cavity height ( $h$ ) is adjusted to control the band gap of EBG which is 60 mm. This S-parameter is plotted in Fig. 12 and shown the band gap at frequency 2.21 GHz to 2.31 GHz.

**Case 2 : Co-polarization of EBG**

The double EBG polar V is considered, a unit cell is surrounded by four periodic boundaries as shown in Fig. 13. This model can estimate the transmission and the reflection wave of the EBG structure as plotted in Fig. 14(a) Consideration of  $S_{11}$  and  $S_{21}$  at 2.1 GHz concludes that the aluminium rod can be partially reflected wave. The reflection phase in Fig. 14(b) is performed that larger phase inversion has been obtained, thus the allowed bandwidth can be increased. Referring to Fig. 15 denoted that the aluminium rods are classified in a medium with epsilon near zero (ENZ) with the permittivity, permeability and refraction index of 0.01, 22.29 and 0.47, respectively. The band gap of the co-polarized EBG is obtained by using the cavity model. Let us now analyze the transmission and reflection coefficient, assuming the cavity height ( $h$ ) is adjusted to control the band gap of EBG which is 60.3 mm. The band gap in Fig. 16, is covering the frequency of 1.83 GHz to 2.25 GHz.

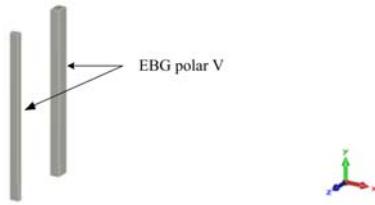
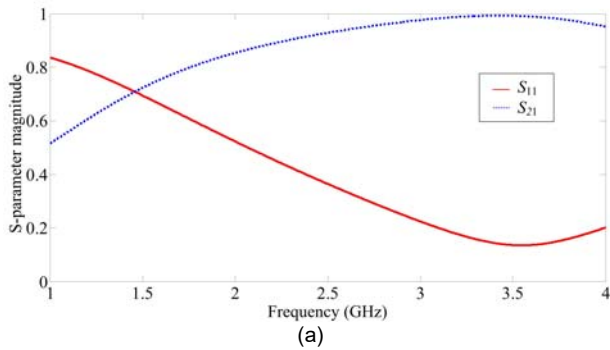
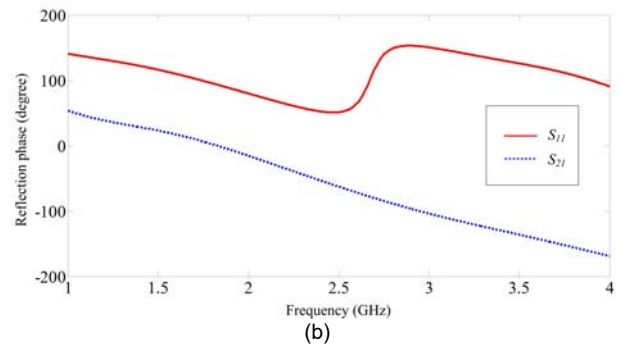


Fig.13. A unit cell of double layers with co-polarization.

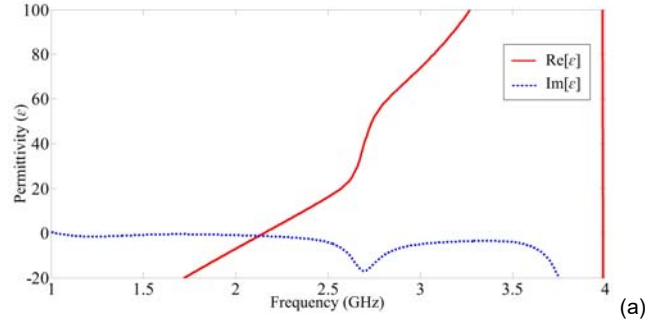


(a)

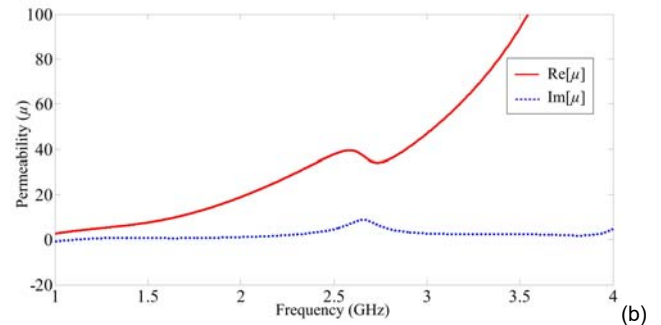


(b)

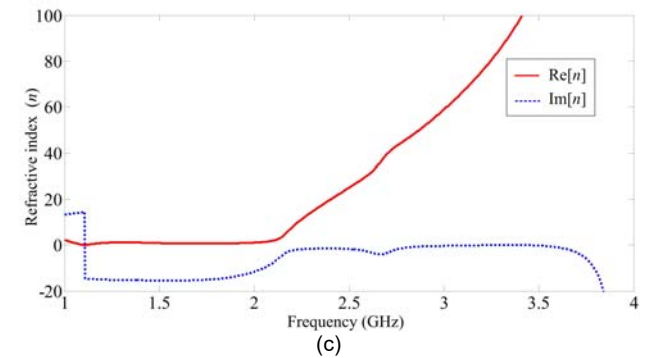
Fig. 14. S-parameter of double layers with co-polarization (a) magnitude and (b) phase.



(a)



(b)



(c)

Fig.15. Calculated results of the double layers with co-polarization (a)  $\epsilon_r$ , (b)  $\mu_r$ , and (c)  $n$ .

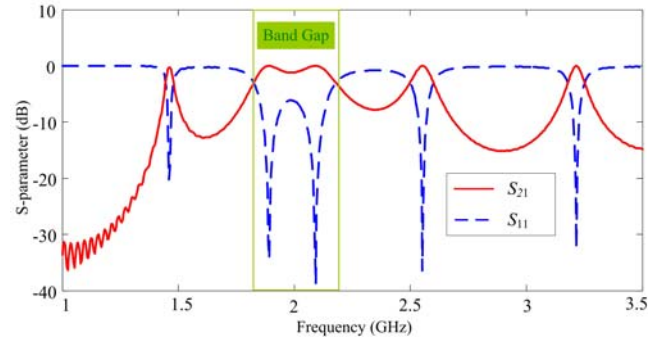


Fig. 16. The band gap of double layers with co-polarization.

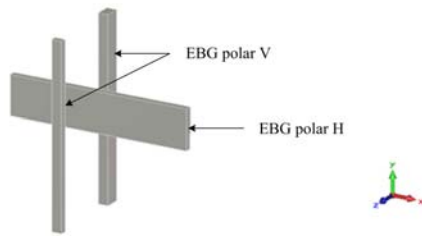


Fig.17. A unit cell of three layers.

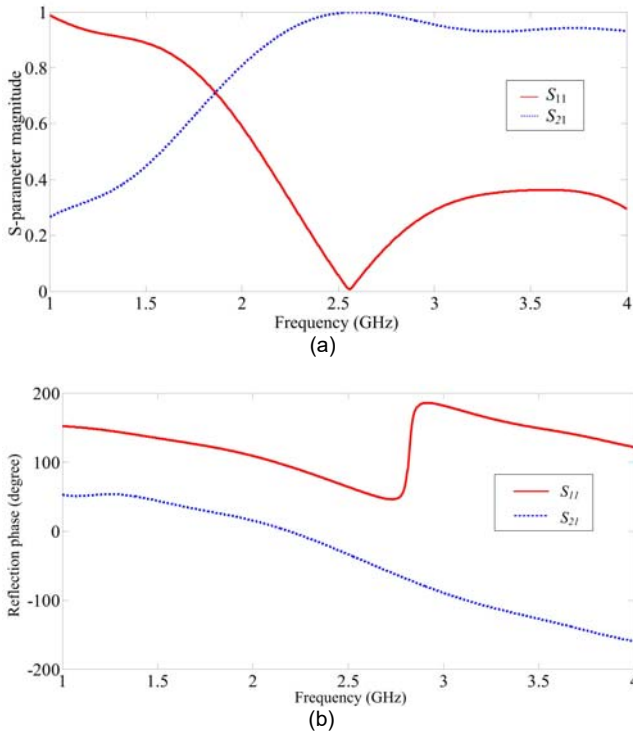


Fig. 18.S-parameter of three layers (a) magnitude and (b) phase.

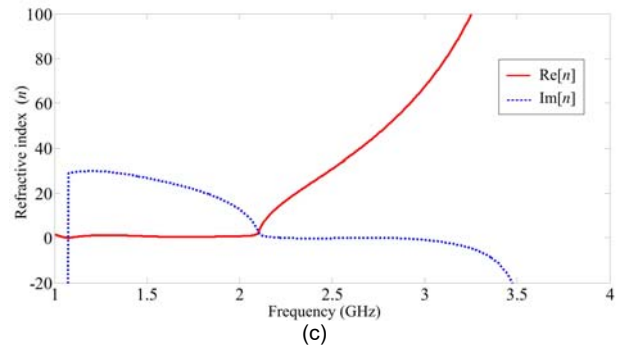
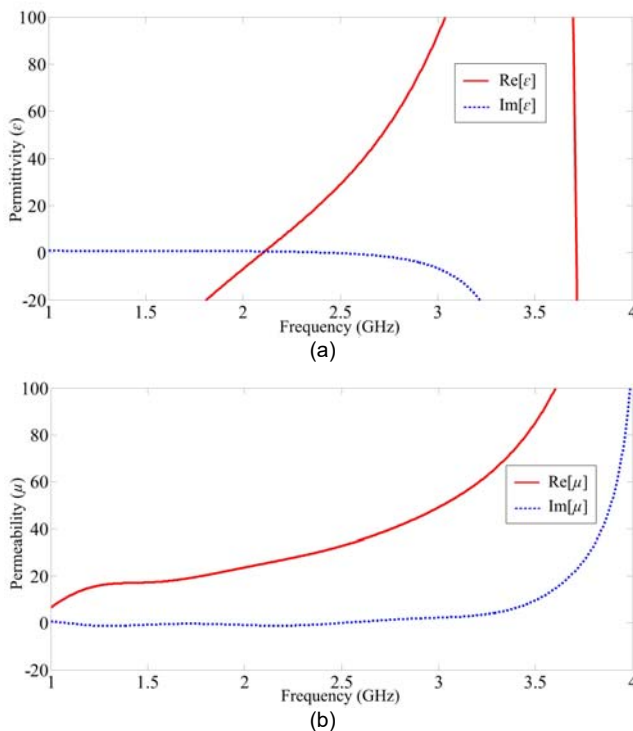


Fig.19. Calculated results of three layers (a)  $\epsilon_r$ , (b)  $\mu_r$ , and (c)  $n$ .

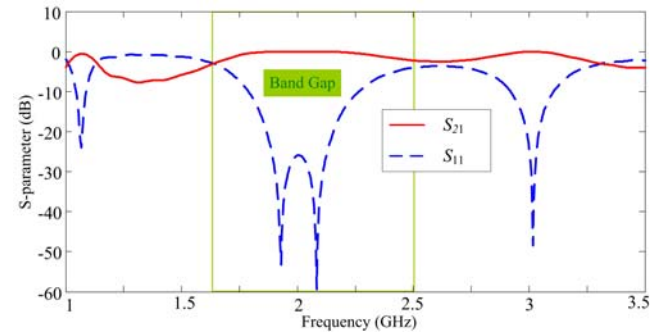


Fig.20. The band gap of three layers.

### Three layers of metallic rod

Three layers are considered and a unit cell is surrounded by four periodic boundaries as shown in Fig. 17. This model can estimate the transmission and the reflection wave of the EBG structure as plotted in Fig. 18(a). Consideration of  $S_{11}$  and  $S_{21}$  at 2.1 GHz concludes that the aluminium rod can be partially reflected wave. The reflection phase in Fig. 18(b) is performed that larger phase inversion has been obtained, thus the allowed bandwidth can be increased. Fig. 19 illustrates the electromagnetic properties of three layers EBG, it is classified in a medium with epsilon near zero (ENZ) with low refraction index of 2.6. The band gap of the three layers EBG is obtained by using the cavity model. Let us now analyze the transmission and reflection coefficient, assuming the cavity height ( $h$ ) is adjusted to control the band gap of EBG which is 60.31 mm. This S-parameter is plotted in Fig. 20, indicate one partially reflected band gap at frequency 1.65 GHz to 2.5 GHz. The resonant bandwidth is increased because the cavity gap from bottom layer to top layer of metallic rods is more than one and double layers.

The characteristic of metallic rods type metamaterials are summarized in Table 1. If the gap between co-polarized layers are increased, the frequency band gap is wide band. The wider resonant band gap occurs in two cases that are double layers with co-polarization case and three layers case. When considering the values that represent the properties of metamaterials, ENZ is appeared when the number of layers of the metallic rods increases, whether cross or co polarization.

Table 1. Characteristic of metallic rods metamaterials

Metallic rods Arrangement	Frequency band gap (MHz)	Classification of metamaterials
Single Layer	100	DPS
Double Layers	Cross	100
	Co	420
Three Layers	900	ENZ

## Conclusion

The aims of this research are classified metamaterials modelling in metallic rod structure. Moreover, the modified structures are analysed its electromagnetic capability such as permittivity, permeability, and refraction index. The single layer metallic rod structure is performed partially reflective surface (PRS) based on metamaterials. It can operate with narrow band gap. In double layers case, the permittivity is near zero and the refraction index is closed to zero, so the directivity enhancement in this medium is based on the phenomenon of geometrical optics and Snell's law. For enhance the bandgap, the third layer of metallic rod is installed. Therefore, the cavity gap from bottom layer to top layer of metallic rods. Furthermore, all of metallic rod arrangement can be achieved EBG and PRS characteristics for applying in antenna engineering.

**Acknowledgment:** Thank you to the department of Telecommunications Engineering, Faculty of Engineering and Architecture, Rajamangala University of Technology Isan for providing support with the equipment. In addition, thank you to School of Electronic Engineering and Telecommunications Engineering, Institute of Engineering, Suranaree University of Technology for supporting this work with the equipment and the CST software.

**Authors:** Assist. Prof. Dr. Nuchanart Santalunai, [E-mail: nuchanart.fa@rmuti.ac.th](mailto:nuchanart.fa@rmuti.ac.th), Department of Telecommunication Engineering, Faculty of Engineering and Architecture, Rajamangala University of Technology Isan, Nakhon Ratchasima, Thailand; Dr. Samran Santalunai, [E-mail: samran.sa@sut.ac.th](mailto:samran.sa@sut.ac.th), School of Electronic Engineering, Suranaree University of Technology, Nakhon Ratchasima, Thailand; Adisak Rattananamlom, [E-mail: M5940622@g.sut.ac.th](mailto:M5940622@g.sut.ac.th), School of Electronic Engineering, Suranaree University of Technology, Nakhon Ratchasima, Thailand; Assist. Prof. Dr. Pichaya Chaipanya, [E-mail: pichayac@g.swu.ac.th](mailto:pichayac@g.swu.ac.th), Department of Electrical Engineering, Srinakharinwirot University, Nakhon Nayok, Thailand; Assoc. Prof. Dr. Piyaporn Meesawad, [E-mail: piyaporn@sut.ac.th](mailto:piyaporn@sut.ac.th), School of Telecommunication Engineering, Suranaree University of Technology, Nakhon Ratchasima, Thailand; . Assoc. Prof. Dr. Chanchai Thongsopa, [E-mail: chan@sut.ac.th](mailto:chan@sut.ac.th), School of Electronic Engineering, Suranaree University of Technology, Nakhon Ratchasima, Thailand; Assist. Prof. Dr. Tajchai Pumpoung, [E-mail: tajchai.pu@rmuti.ac.th](mailto:tajchai.pu@rmuti.ac.th), Department of Telecommunication Engineering, Faculty of Engineering and Architecture, Rajamangala University of Technology Isan, Nakhon Ratchasima, Thailand

## REFERENCES

- [1] Lier E., Shaw R.K., Design and simulation of metamaterial-based hybrid-mode horn antennas, *Electronics Letters*, 44 (2008), no. 25, 1444-1445
- [2] Xiong H., Hong J.-S., Tan M.-T., Li B., Compact microstrip antenna with metamaterial for wideband applications, *Turkish Journal of Electrical Engineering and Computer Sciences*, 21 (2013), no. 2, 2233-2238
- [3] Ozturk Y., Yilmaz A.E., Multiband and perfect absorber with circular fishnet metamaterial and its variations, *Applied Computational Electromagnetics Society Journal*, 31 (2016), no. 12, 1445-1451
- [4] Liu C., Zha S., Liu P., Yang C., Zhou Q., Electrical manipulation of electromagnetically induced transparency for slow light purpose based on metal-graphene hybrid metamaterial, *Applied Sciences (Switzerland)*, 8 (2018), no. 12, 2672
- [5] Lyu S., Qin B., Deng H., Ding X., Origami-based cellular mechanical metamaterials with tunable Poisson's ratio: Construction and analysis, *International Journal of Mechanical Sciences*, 212 (2021), 106791
- [6] Chen Z., Qu F., Wang Y., Nie P., Terahertz dual-band metamaterial absorber for trace indole-3-acetic acid and tricyclazole molecular detection based on spectral response analysis, *Spectrochimica Acta - Part A: Molecular and Biomolecular Spectroscopy*, 263 (2021), 120222
- [7] Wang H., Pan C., Zhao H., Wang T., Han Y., Design of a metamaterial film with excellent conformability and adhesion for bandage substrates, *Journal of the Mechanical Behavior of Biomedical Materials*, 124 (2021), 104799
- [8] Kumar A., Rajawat M.S., Mahto S.K., Sinha R., Metamaterial-Inspired Complementary Split Ring Resonator Sensor and Second-Order Approximation for Dielectric Characterization of Fluid, *Journal of Electronic Materials*, 50 (2021), no. 10, 5925-5932
- [9] Wang H., Zhao D., Jin Y., Wang M., Mukhopadhyay T., You Z., Modulation of multi-directional auxeticity in hybrid origami metamaterials, *Applied Materials Today*, 20 (2020), 100715
- [10] Willie J.P., Dimitri N.B., David R.S., Negative refractive index metamaterials, *Materials Today*, 9 (2006), no. 7-8, 28-35
- [11] Engheta N., Ziolkowski R. W., In the literature, most widely used designations are "double negative" and "left-handed", *Metamaterials, Physics and Engineering Explorations*, (2006), Wiley & Sons. Chapter 1.
- [12] Budnarowska M., Mizeraczyk J., The numerical simulation of the interaction of a plane electromagnetic wave with a metasurface consisting of split-ring resonator, *Przeglad Elektrotechniczny*, 97 (2021), no. 3, 39-42
- [13] Das G.K., Basu S., Mandal B., Augustine R., Mitra M., Gain-enhancement technique for wearable patch antenna using grounded metamaterial, *IET Microwaves, Antennas and Propagation*, 14 (2020), no. 15, 1983-1989
- [14] Roy M., Mittal A., Surface Wave Suppression in LHCP Microstrip Patch Antenna Embedded on Textured Pin Substrate, *Progress In Electromagnetics Research C*, 89 (2019), 171-180
- [15] Guelber E.F., Cardoso A.S.V., Capovilla C.E., Araujo H.X., A modified ultra wide band antenna with metamaterial patterns for telecommunications systems, *Przeglad Elektrotechniczny*, 92 (2016), no. 1, 166-169
- [16] Rudyk K., Kubacki R., Lamari S., The microstrip antenna with metamaterial property, *Przeglad Elektrotechniczny*, 92 (2016), no. 12, 149-152
- [17] Kamil A., Mohammad M., Babar M., Edl S., Kevin J.M., The Effects of an Electromagnetic Crystal Substrate on a Microstrip Patch Antenna, *IEEE Transactions on antennas and propagation*, 50 (2002), no. 4, 451-456
- [18] Zhendong D., Dan Z., Chunyu M., A Study of a Microstrip Patch Antenna With a Drilled Through-Holes Array Structure Based on the Line Source Analysis Method, *Frontiers in Physics*, 8 (2020), 290
- [19] Contopanagos H.F., A broadband polarized artificial magnetic conductor metasurface, *Journal of Electromagnetic Waves and Applications*, 30 (2020), no. 14, 1823-1841
- [20] Taixia S., Lijuan D., Yongqiang C., Yong S., Yanhong L., Fusheng D., Lixiang L., Yunlong S., Yanyan S., Using artificial magnetic conductors to improve the efficiency of wireless power transfer, *AIP Advances*, 9 (2019), 045308
- [21] Das G.K., Das G.K., Basu S., Mandal B., Mitra D., Augustine R., Mitra M., Gain-enhancement technique for wearable patch antenna using grounded metamaterial, *IET Microwaves, Antennas and Propagation*, 14 (2020), no. 15, 1983-1989
- [22] Pei R., Leach M.P., Lim E.G., Wang Z., Song C., Wang J., Zhang W., Jiang Z., Huang Y., Wearable EBG-Backed Belt Antenna for Smart On-Body Applications, *IEEE Transactions on Industrial Informatics*, 16 (2020), no. 11, 7177-7189
- [23] Amalraj T.D., Savarimuthu R., Design and Analysis of Microstrip Patch Antenna Using Periodic EBG Structure for C-Band Applications, *Wireless Personal Communications*, 109 (2019), no. 3, 2077-2094
- [24] Weily A.R., Horvath L., Esselle K.P., Sanders B.C., Bird T.S., A planar resonator antenna based on a woodpile EBG material, *IEEE Transactions on Antennas and Propagation*, 53 (2005), no. 1, 216 - 223
- [25] Markad N.T., Kanphade R.D., Wakade D.G., Design of Cavity Model Microstrip Patch Antenna, *Computer Engineering and Intelligent Systems*, 6 (2015), no. 4, 1-15
- [26] Richard W.Z., Design, Fabrication, and Testing of Double Negative Metamaterials, *IEEE Transactions on antennas and propagation*, 51 (2003), no. 7, 1516-1529
- [27] David A. A., Charman W.N., Thomas Young's contributions to geometrical optics, *Clinical and Experimental Optometry*, 94 (2011), no. 4, 333-340